國 立 清 華 大 學

碩士論文

在 MonoHbb 分析中的 W 玻色子背景估計

The Estimation of the Background of the W Boson in the MonoHbb Analysis

系　　　所：物理研究所

學　　　號：105022511

研 究 生：韓正忻　　　　(Cheng-Hsin Han)

指導教授：徐百嫻　博士　(Prof. Pai-Hsien Jennifer Hsu)

中 華 民 國 一○七 年 十二 月

Todo list

"Todo List" will hide when set \setboolean{publish}{*true*} in config.tex.

在 MonoHbb 分析中的 W 玻色子背景估計

摘要

在此寫上你的中文摘要。

關鍵字：關鍵字, 論文, 樣板, 讓我畢業

摘要

摘要

The Estimation of the Background of the W Boson in the MonoHbb Analysis

Abstract

Write your English abstract here.

Keywords: Keyword, Thesis, Template, Graduate me

ABSTRACT

Acknowledgement

Thanks NCU, and sppmg's LATEX template__**sppmg/tw__thesis__template__????**.

ACKNOWLEDGEMENT

Contents

List of Figures

List of Tables

LIST OF TABLES

Glossary

Use table for symbol list. You can also use package "nomencl" (simple) or "glossaries" (powerful). see packages document or my tutorial (but it's Chinese).

Glossary

VIM	:	The best guy's editor
Emacs	:	The God's editor
CTAN	:	Comprehensive TeX Archive Network, ctan.org

GLOSSARY

Chapter 1

Introduction

(You can copy "chapter_template.tex" or "chapter_template_demo.tex" to create new sub-file(chapter).)

Write your Introduction here. eg,

I don't want my chaste thesis impinge by M$. But LaTeX is little hard.

Chapter 2

The ATLAS detector

2.1 Coordinates

The ATLAS (**A T**oroidal **L**HC **A**pparatu**S**) experiment is one of the seven detector in Large Hadron Collider (LHC) at CERN (European Organization for Nuclear Research). Its cylindrical symmetry and end caps covers nearly 4π in solid angle.

A coordinate system is used to describe every recorded signals nearby. The origin is set at the center of the detector, or the interaction point (IP). The x-axis points toward the center of the LHC ring; the y-axis points vertically upward; the z-axis points along one of the beam pipe direction such that a right-handed coordinate sysetem is created.

A modified version of cylindrical coordinate is more commonly used in the experiment. The pseudorapidity $\eta \equiv -\ln\tan(\theta/2)$, in which θ is the polar angle in cylindrical coordinate, is used to decribe the angle between the z-axis and the direction of interest. (r, ϕ) is the same system to describe the tranverse plane, with ϕ being the azimuthal angle. In addition, the cone size variable, which is used in object selection and reconstruction, is defined as $\Delta R \equiv \sqrt{(\Delta\phi)^2 + (\Delta\eta)^2}$.

2.2 Components of ATLAS

Depending on its function, the components are categorized into four parts - inner detector, calorimeters, muon spectrometer, and the magnetic system. Apart from these, there are three levels of triggers which are designed to reduce the amount of data and also keep the signals of interest. Figure 2.1 shows the schematic positions and 2.2 shows

the side view of each components of ATLAS. The solenoidal magnets surround the inner detector while the toroidal magnets affects the signals in the muon spectrometer. These two magnets form the magnetic system. The others consist of smaller layers or components which is described in the following.

Figure 2.1: Schematic plot of the ATLAS detector as well as the positions of its components.

Figure 2.2: Schematic plot of the side view of the ATLAS detector.

2.2.1   Inner Detector

The inner detector begins few centimeters from the IP. Its main function is to track the trace of charged particles by their interations with the materials. A 2T magnetic field, which is generated from the solenoidal magnets surrounding the whole inner detector, causes the charged ones to bend. Based on the directions and the curvatures, one can determine their charge and momentum preliminarily. The inner detector comprises three parts - the pixel detector, the semi-conductor tracker (SCT), and the transition rediation tracker (TRT).

The pixel detector is located at the innermost part of the inner detector. It contains four layers of modules, which is made up silicon, in the direction perpendicular to the beam. It covers pseudorapidity range $|\eta| < 2.5$ and its proximity to the IP is meant to measure extremely precise trace of the charged particles. Three disks, which are made up of similar material, are at each end cap of the detector.

The semi-conductor tracker has a similar concept and function to the pixel detector. It lies in the middle part of the inner detector. The SCT is in a long and narrow strip-shape rather than small pixels and covers the perpendicular directions to the beam instead of nearly full coverage. The SCT overlays a larger area than the pixel detector does. Therefore, it has more sampled points and is of great importance on tracking the transverse directions with roughly the same accuracy compared to the pixel detector.

TRT is the outermost component. It includes straw tube trackers and transition radiation detectors. Its precision in tracking is not as high and its coverage in pseudorapidity, about $|\eta| < 2.0$, is not as wide as those of the other two components. However, TRT possesses transition radiation detection capability, which is useful for identifying charged particles. Lighter particles tend to have higher speed, which generates greater transition radiation. Thus, electrons and positrons, the lightest charged particles, would leave strong signals in TRT.

2.2.2   Calorimeters

Outside the solenoidal magnet, which envelops the inner detector, are the calorimeters. By absorbing the particles, the calorimeters measure the energies of them. Two layers of components compose the calorimeter systems, the inner electromagnetic (EM) calorimeter

and the outer hadronic calorimeter.

As its name suggests, the EM calorimeter absorbs energies from particles that interact electromagnetically, including photons and charged particles. High-granularity lead/liquid argon(LAr) EM calorimeter covers a range of $|\eta| < 3.2$, which includes the barrel and end cap. In addition, a LAr persampler which is meant to correct the energy loss in materials of the calorimeters covers $|\eta| < 1.8$. For the forward region, which has the range $3.1 < |\eta| < 4.9$, a LAr EM calorimeter with copper is also deployed.

Hadronic calorimeter is less precise in both energy magnitude and localization than EM calorimeter. It absorbs energies from the particles that interact via strong force. Hadrons and τ leptons, which are identified as jets, are the targeted particles of hadronic calorimeter. Steel/scintillator-tile covering $|\eta| < 1.7$, two copper/LAr end cap calorimeters overlaying $1.5 < |\eta| < 3.2$, and a forward-regional ($3.1 < |\eta| < 4.9$) tungsten absorbers constitute the hadronic calorimeter.

2.2.3 Muon Spectrometer

Muon spectrometer, which is meant to provide more precise measurement of muon momentum and tracks, surrounds the calorimeters. Due to the fact that almost only muons pass reach it, muon spectrometer also has a function of identifying the muons. A magnetic field, provided by three toroidal magnets and thus is not uniform, creates a curve in muon tracks. These tracks can be made use of measuring the momentum. Detectors with triggers provide the identification and momentum measurements of the muons within the range $|\eta| < 2.4$; over a thousand precision tracking chambers covering $|\eta| < 2.7$ serve the muon spatial measurements.

2.2.4 Trigger System

A trigger is a set of device which sets thresholds on some physical quantities such as momenta and positions. If the threshold of one event is met, one keeps it; otherwise one abandons it. The ATLAS triggers consist of three levels. The first level is hardware based while the other two are software based. From roughly 1 billion events per second, these three levels of triggers combined select about few hundreds interesting. Namely, the interaction rate is reduced from 1 GHz to few hundreds Hz.

Chapter 3

Object Selection and Reconstruction

Signals recorded in the ATLAS detector are categorized or reconstructed as pysical objects, which could be further used in the analyses. Besides the head-to-head (or hard-scattered) events which have high transverse momentum (p_T) there are also additional collisions with lower p_T. These are referred to as the pile-up events, which one often wants to exclude in the analyes. The reconstruction and definition of objects used in this study are listed in the following.

3.1 Jets

Jets are the reconstruction of collimated bunches of hadrons. In ATLAS experiment, the anti-k_T algorithm is usually used to recombine hadrons into cone-sized shapes. In short, the anti-k_T algorithm makes use of p_T of each given entities and reconstructs jets whose R is the given radius parameter and which center on hard-scattered particles. How the jets are reconstructed and defined in this study is tabulated in table.3.1 and explained as follows.

Table 3.1: Summary of the jet selection and reconstruction.

type	(*central*) small-R jets	(*forward*) small-R jets	large-R jets	VR track jets
p_T (GeV)	> 20	> 30	> 200	> 0.5
$\|\eta\|$	(0, 2.5)	(2.5, 4.5)	(0, 2.0)	(0, 2.5)
R	0.4		1.0	$\rho/p_T \in (0.02, 0.4)$ with $\rho = 30$ GeV
additional	if $\|\eta\| < 2.4$ then $p_T < 60$ GeV	-		$\|z_0 \sin(\theta)\| < 3$ mm

3.1.1 Small-radius Jets

Small-radius (small-R) jets have a relative smaller size compared to large-radius (large-R) jets, which would be discussed in subsection 3.1.2. They are main feature when the missing transverse momentum (E_T^{miss}, discussed in section 3.3) is below a certain value (see section 4.1).

Using the anti-k_T algorithm with a raidus parameter of 0.4 small-R jets can be reconstructed from the energy deposits in the calorimeter. Small-R jets are further categorzied into two types, the central jets and the forward jets. Central small-R jets are those within $|\eta| < 2.5$ and whose $p_T > 20$ GeV. Forward small-R jets are within $2.5 < |\eta| < 4.5$ and are required of a p_T threshold of greater than 30 GeV. For jets in $|\eta| < 2.4$, an additional threshold of $p_T < 60$ GeV is require. To further suppress these jets from the pile-up interactions, they are required to be originated from the reconstructed location of the collision, or the primary vertex. In addition, jets containing b-quark are referred to as b-jets. The method used to identify them as b-jets are called b-tagging. Because b-quarks have a relative longer lifetime compared to other particles, they would emit from a secondary vertex rather than the primary one, which can be made use of to perform the b-tagging. A working point of 77% on averge for the b-tagging efficiency is used in this analysis.

3.1.2 Large-radius Jets

Large-R jets have a relative larger size compared to small-R jets, which is covered in the last subsection. They are the characteristic objects when the E_T^{miss} exceeds a threshold value (see section 4.1). Usually they are associated with variable-radius (VR) jets, which will be covered in subsection 3.1.3.

The large-R jets are reconstructed via the anti-k_T algorithm with a radius parameter of 1.0. The reconstruction highly depends on the calorimeter and the tracking system. Certain calibration method is appiled for the energy deposits in the calorimeter. The calibrated jets have a p_T threshold of 200 GeV and are required to be within the range of $|\eta| < 2.0$.

3.1.3 Variable-radius Jets

The large-R jets are a result of two "merged" small jets. In order to identify the small jets inside the reconstructed large-R jets, the VR track jets are introduced.

The VR track jets are also reconstructed using the anti-k_T algorithm. Those jets whose p_T does not exceed 0.5 GeV or out of the range of $|\eta| < 2.5$ are not considered. To suppress the pile-up jets, a creiteria on the longitudinal impact parameter, $|z_0 \sin(\theta)| < 3$ mm, is required. In this, z_0 is the point closet to the vertex along the logitudinal axis and θ is the polar angle of the track. The main feature of the VR track jets is that the radius parameter depends on the value of p_T rather than a constant value:

$$R \to R_{\text{eff}}(p_T) \approx \frac{\rho}{p_T}, \tag{3.1}$$

in which ρ is set at 30 GeV, which is the optimal value ragarding the efficiency for b-tagging. The upper limit and lower limit, $R_{\max}$ and $R_{\min}$ are set at 0.4 and 0.02 in this regard.

3.2 Leptons

Leptons are used to categorized the regions selected in this analysis, which would be covered in chapter 4. Requirements of each flavor are explained in the following and summarized in table.3.2.

Table 3.2: Summary of lepton selection and reconstruction. The rightmost column are the requirements for the reconstructed small-R jet that decays from a τ-lepton candidate. The parentheses in the cell of μ ID would be covered in the next chapter.

flavor	e		μ		τ
categorization	baseline	signal	baseline	signal	-
p_T (GeV)	> 7	> 27	> 7	> 25	> 20
$|\eta|$	(0, 2.47)		(0, 2.7)	(0, 2.5)	$(0, 1.37) \cup (1.52, 2.5)$
ID	Loose		Loose (0/2-lepton) Medium (1-muon)		Loose
transverse impact parameter	$d_0/\sigma(d_0) < 5$		$d_0/\sigma(d_0) < 3$		$|d_0| < 1$ mm
$|z_0 \sin(\theta)|$ (mm)	< 0.5				< 1.5
Additional	-				one to four track-jets $\Delta\phi(\tau, E_T^{\text{miss}}) < \frac{\pi}{8}$

3.2.1 Electrons

Electron candidates are reconstructed from the energy deposits in EM calorimeter that match a track recorded in the inner detector. All candidates within $|\eta| < 2.47$ are considered. In addition, there is a LLH-based algorithm, which further makes use of multivariable analysis (MVA), applied for the electron ID. Three levels of ID operating point, loose, medium and tight, are povided; among them, loose ID is used in this study for the electrons. Requirements of the impact parameter are examined, both in the transverse and logitudinal directions. For the former, the relative resolution, which is the fraction of the transverse impact parameter d_0 and its resolution $\sigma(d_0)$, has an upper bound of 5. For the latter, the value $|z_0 \sin(\theta)| < 0.5$ mm is set.

Electrons are divided into two groups. The baseline electrons are those whose p_T exceed 7 GeV. The signal electrons, which require a tighter threshold of $p_T > 27$ GeV, are the other groups. The purpose of this categorization is to label which electrons decay more likely from heavier particles. Therefore, it can be used as a sign of different analysis regions. More details of these regions can be found in chapter 4.
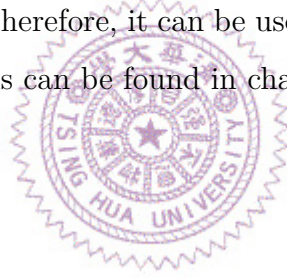
3.2.2 Muons

Muon candidates, also divided into baseline and signal muons, are reconstructed with high dependence of inner detector and the muon spectrometer. The purpose of the categorization is the same as that of the electrons. Signal muons are those whose p_T exceed 27 Gev. Also, one needs to have more acurate identification of the signal muons compared to the baseline ones. They are required to leave tracks in the inner detector, and thus shall be found in $|\eta| < 2.5$. For baseline muons, which have a looser p_T threshold of 7 GeV, an acurate identification is not sufficient. Therefore, leaving signals in the inner detector is not required. Their pseudorapidity range are set within $|\eta| < 2.7$, which is the range of the muon spectrometer.

On top of that, the impact parameter must be consistent with the the primary vertex. $d_0/\sigma(d_0) < 3$ and $|z_0 \sin(\theta)| < 0.5$ mm are set. Finally, a loose ID is used for the zero-lepton and two-lepton channel whilst the one-muon channel makes use of a medium ID for the muons in this analysis. These channels would be covered in the upcoming chapter.

3.2.3   Taus

τ-leptons, whose decay length is few μm, barely reach the ATLAS detector and thus are mainly reconstructed from their decay products. Due to the fact that most of the τ-leptons decay into hadrons, the τ-lepton candidates are reconstructed from jets. The transverse impact parameter, $|d_0| < 1$ mm, and the logitudinal one, $|z_0 \sin(\theta)| < 1.5$ mm, are set for the jet tracks and the τ vertex. The threshold on the p_T of the jets is set at 20 GeV; the range of $|\eta| < 2.5$, excluding $1.37 < |\eta| < 1.52$. The excluded region is those between the barrel and the forward region, or the crack region. Furthermore, the ID is built on a boosted decision tree (BDT) that makes use of the information from the tracks and the calorimeter. The loose working point on the τ-leptons is used. Finally, the small-R jet is required to contain one to four track-jets and within a range of $\Delta\phi < \frac{\pi}{8}$ with the missing transverse energy (E_T^{miss}, see section 3.3) in order to suppress the W-boson-decayed τ-leptons.

3.3   Missing Transverse Momentum

The missing transverse momentum is the imbalance in p_T of the reconstructed objects. Thus, it can be reconstructed as the negative vector transverse momentum sum. This includes the hard-scattered objects and the soft term. The momentum of hard-scattered reconstructed particles construct the former. As for the soft term, tracks that are not associated to any reconstructed hard objects are considered. The vetoed leptons, which are the leptons that needs to removed from the analysis in some channels, which would be covered in the next chapter, also count as the soft term. Jets that failed the selection of small-R jets also contributes the soft term, with the p_T threshold on the forward small-R jet being modified to 20 GeV. The absolute value of the missing transverse momentum is denoted as E_T^{miss}.

An estimation variable E_T^{miss} significance, S, is used to check the genuinity in whether E_T^{miss} comes from undectable particles instead of mismeasurements or any inefficiencies. There are two types of E_T^{miss} significance, the event-based one and the object-based one. The former one is the ratio of the E_T^{miss} and the square root of the transverse momentum

of hard-scattered particles, H_T, i.e.,

$$S_{\text{event}} = \frac{E_T^{\text{miss}}}{\sqrt{H_T}}, \tag{3.2}$$

where

$$H_T = \Sigma p_T^\mu + \Sigma p_T^e + \Sigma p_T^\gamma + \Sigma p_T^\tau + p_T^{\text{jets}}. \tag{3.3}$$

If the soft term contributes little in the transverse momentum, the value of H_T would be approximately that of E_T^{miss}, and thus the value of E_T^{miss} significance tends to be small. It would be used in the background estimation mainly and would be used as cut in the next chapter.

The other significance value, the object-based one, is a log-likelihood ratio value. It is used to test the hypothesis that the total momentum of the invisible particle is zero against the hypothesis that it is not. In short, if the value of the object-based significance, S_{object} which is non-negative, is close to zero, then it implies high possibilities that E_T^{miss} does not come from the invisible particles; if the value is large, then it implies a possibility of existing invisible particles.
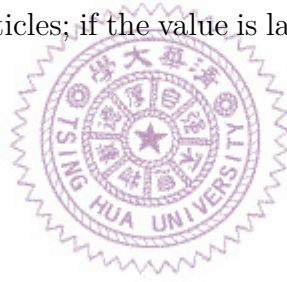
3.4 Overlap Removal

Object ambiguities happen when objects match multiple reconstruction criteria. In the following listed specific steps of object reconstruction that are required to solve the problem.

1. If two electron candidates share the same track, remove the one with lower p_T.

2. If a τ-lepton candidate lies within $\Delta R = 0.2$ of an electron or muon, it is removed.

3. Reject the electron candidates whose track is shared with a muon candidate.

4. Small-R jets are removed if they are within $\Delta R = 0.2$ of an electron.

5. Remove the electrons that are within $\Delta R = \min(0.4, 0.04 + 10\text{GeV}/p_T^{\text{electron}})$ of a small-R jet.

6. If the separation between a small-R jet and a muon is within $\Delta R = 0.2$, the small-R jet is removed provided that it has fewer than three tracks or that the muon p_T is

greater than 50% of the jet p_T and is greater than 70% of the p_T sum of the tracks associated to the jets.

7. Remove the muons that are within $\Delta R = \min(0.4, 0.04 + 10\text{GeV}/p_T^{\text{muon}})$ of a small-R jet.

8. Large-R jets whose track is within $\Delta R = 0.1$ to that of an electron are removed.

Chapter 4

Event Selection

A number of selection is applied on the events in this study. Because the final state of the Z'-2HDM model contains no leptons (see fig. 4.1), one can define this zero-lepton region as the signal region (SR). However, there are other processes having the same final products as that of this model, which is recognized as the background. To further estimate the amount of the background events, one analyzes other processes that are similar to the background. These processes are called the control region (CR). Both SR and CR are discussed in this chapter. Some comparisons and characteristic selections of SR and CRs are summarized in table 4.1.
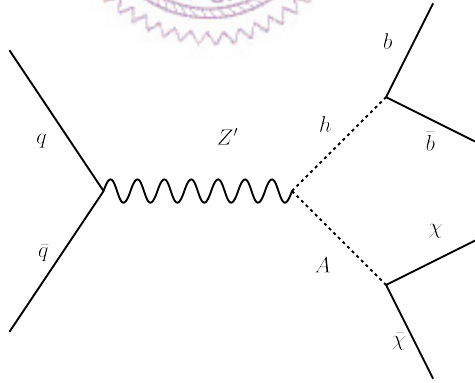
Figure 4.1: The Feynman diagram of the Z'-2HDM model.

4.1 Signal Region

First, no baseline leptons candidates, including the τ-leptons, are considered. The value of E_T^{miss} is required to be at least 150 GeV. Multijet backgrounds may pass the selection criteria. To further suppress this background, one adds two selections. The

first one requires the azimuthal angle between E_T^{miss} and any of the three highest-p_T jets $(\min(\Delta\phi(E_T^{\text{miss}}, \text{jet})))$ greater than 20°. The forward jets are only considered if the number of central jets is less than 3. The other selection requires the azimuthal angle between E_T^{miss} and p_T^{miss} smaller than 90°, where p_T^{miss} is the negative sum of object momentum measured by the inner detector.

After these selections, one devides these events into two regions based on the value of E_T^{miss}. Those whose E_T^{miss} is smaller than 500 GeV are defined as the resolved region, whilst the merged region contains those events with $E_T^{\text{miss}} > 500$ GeV. The resolved region are further divided into three regions, whose E_T^{miss} are within $(150, 200]$, $(200, 350]$, and $(350, 500]$. Different sets of selections are applied in these two regions and tabulated in table 4.2.

For the resolved region, the events are required to have at least two small-R jets, which is the reason of the naming of this region. In these jets, exactly two b-tagged jets are also required. The p_T of one of the jets has to exceed 45 GeV. For the events with two (three or more) jets, the scalar sum of the p_T of the highest two (three) jets is also required to be at least 120 (150) GeV. A requirement of $S_{\text{object}} > 16$ is also applies. To further suppress the multijet backgrounds, a selection on the separation are required. Due to the conservation of the momentum, one expects the tracks of the E_T^{miss} and the Higgs candidate are back-to-back. The azimuthal angle between E_T^{miss} and the Higgs candidate is required to be greater than 120°. The azimuthal angle between the two jets from the Higgs candidate $(\Delta\phi(\text{jet}_1, \text{jet}_2))$ tends to be large in multijet background events because of the topology. Thus, it is required to be smaller than 140° in this study. Furthermore, in order to reject $t\bar{t}$ background events, two more selections are added. One of them is $\Delta R(\text{jet}_1, \text{jet}_2) < 1.8$. The scalar sum of the first three highest p_T of the jets is required to be greater than 63% of the scalar sum of all jets is considered as the other one. At last, one adds a Higgs mass window selection on the two b-tagged jets, 50 GeV $< m_{\text{jj}} < 280$ GeV.

As for the merged region, the events which contains at least one large-R jets are considered, which is the reason of the name "merged". The large-R (VR track) jet with the highest p_T are referred to as the leading large-R (VR track) jet. Two leading VR track jets associated with the leading large-R jet are required be to b-tagged. Events with any VR track jets outside the large-R jets are rejected. To suppress the $t\bar{t}$ background events,

the value of p_T of the leading large-R jet is required to exceed 43% of the scalar sum of the p_T of the leading large-R jets and all small-R jets. Finally, the invariant mass of the large-R jet is also required to be within a Higgs mass window, 50 GeV $< m_J <$ 270 GeV.

4.2 Control Region

Events containing leptons are used to define the CRs. One makes use of the CRs to estimate the main backgrounds of the Z'-2HDM model shown in fig. 4.1. These main backgrounds are shown in 4.2. Based on the number of leptons, the background events can be further categorized into two CRs. The $t\bar{t}$ and W+jets production are estimated from the 1-muon CR. The 2-lepton CR is used for the Z-jets events analyses.
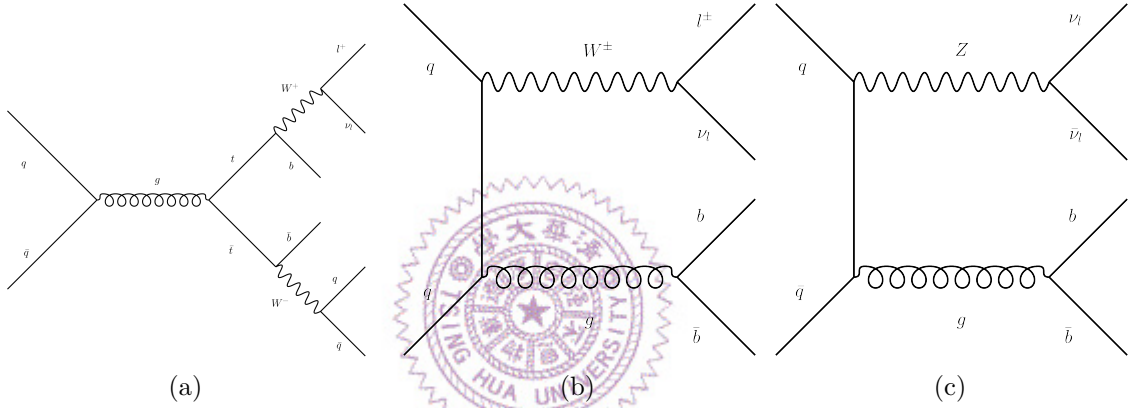

Figure 4.2: The Feynamn diagram of the main background events of the Z'-2HDM model. From left to right, (a) shows the $t\bar{t}$; (b) shows the W+jets events; (c) shows the Z+jets events. For the $t\bar{t}$ events, the lepton could also decay from the W$^-$ boson, which is not shown in this figure.

4.2.1 1-muon Control Region

Although there are leptons in figure 4.2 (a) and (b), these events become the backgrounds because of misidentification or missed detections. As a result, the misidentified or undetected leptons would contribute to the E_T^{miss}. The 1-muon CR is made use of estimating the backgrounds of these $t\bar{t}$ and W+jets events.

Because of the relatively higher fake rate of identification, single electron events are not considered in this background estimation. Therefore, no baseline electrons and exactly one signal muon are required. To mimic how these background events in SR behave, a "proxy" missing transverse momentum is defined as the sum of E_T^{miss} and the transverse

momenta of the muon, or $E_T^{\text{miss,no }\mu}$. The resolved and merged region are also defined using the threshold of 500 GeV on $E_T^{\text{miss,no}\mu}$. Other selections are the same as those mentioned in section 4.1 except the S_{object} selection in the resolved region.

4.2.2   2-lepton Control Region

The neutrinos in figure 4.2 (c) cannot be detected and thus are part of the contributions to the E_T^{miss}. The 2-lepton CR serves as the estimation of this background.

Two same-flavor leptons are required first. For both two-electron or two-muon cases, one lepton is required to be the signal one while the other has to pass the criteria of the baseline one. Additional requirement for the two-muon case is to have opposite charge. In order to make sure that the lepton pair truly decay from the Z boson candidate, a dilepton mass window is applied. The requirement on invariant mass of the two-electron (muon) system is 83 GeV $< m_{\text{ee}} <$ 99 GeV (71 GeV $< m_{\mu\mu} <$ 106 GeV). The "proxy" missing transverse momentum is the absolute value of the sum of the transverse momentum of the two-leptons, or p_T^{ll}. One makes use of p_T^{ll} to define the resolved merged region based on the 500 GeV boundary. Those selections stated in section 4.1 except the S_{object} selection in the resolved region are applied. Apart from that, in order to reduce the $t\bar{t}$ and single top background in this CR, the S_{event} is required to be less than 3.5 GeV$^{\frac{1}{2}}$.

Table 4.1: Comparison of signal region and two control regions. This table only shows the characteristic selections and different definitions of (proxy) missing transverse momentum in different regions. One should combine the selections summarized in table 4.2 to get the whole set of selections in a certain region.

region	signal region	1-muon control region	2-lepton control region
lepton selection	no loose leptons	one signal muon no baseline electrons	two baseline muons or electrons one of them being signal
(proxy) missing transverse momentum	E_T^{miss}	$E_T^{\text{miss,no }\mu} = E_T^{\text{miss}} + p_T^\mu$	p_T^{ll}
E_T^{miss} significance selection (resolved only)	$S_{\text{object}} > 16$	-	$S_{\text{event}} < 3.5$ GeV$^{\frac{1}{2}}$
additional	-	-	83(99) GeV $< m_{\text{ee}(\mu\mu)} <$ 99(106) GeV opposite muon charge

Table 4.2: Summary of common selections of resolved and merged region for all SR and CRs. One should combine the characteristic selections stated in 4.1 to get the whole set of selections in a certain region.

resolved	merged
τ-veto	
$\min(\Delta\phi(E_T^{\mathrm{miss}}, \mathrm{jet})) > 20°$	
$\Delta\phi(E_T^{\mathrm{miss}}, p_T^{\mathrm{miss}}) < 90°$	
(proxy) $E_T^{\mathrm{miss}} \in (150, 500]$ GeV	(proxy) $E_T^{\mathrm{miss}} \in (500, \infty)$ GeV
≥ 2 b-tagged small-R jets	≥ 1 large-R jet
$\Delta R(\mathrm{jet}_1, \mathrm{jet}_2) < 1.8$	$\Delta R(\mathrm{VR}_1, \mathrm{VR}_2) > R_{\min}$
$p_T^{\mathrm{jet}_1} > 45$ GeV or $p_T^{\mathrm{jet}_2} > 45$ GeV	-
$\sum_{i=1}^{2(3)} p_T^{\mathrm{jet}_i} > 120(150)$ GeV	-
$\Delta\phi(E_T^{\mathrm{miss}}, h) > 120°$	-
$\Delta\phi(\mathrm{jet}_1, \mathrm{jet}_2) < 140°$	-
$\sum_{i=1}^{3} p_T^{\mathrm{jet}_i} / \sum_{i=1}^{\infty} p_T^{\mathrm{jet}_i} > 0.63$	$p_T^{\mathrm{large-Rjet}} / (p_T^{\mathrm{large-R\ jet}} + \sum p_T^{\mathrm{small-R\ jet}}) > 0.43$
50 GeV $< m_{\mathrm{jj}} < 280$ GeV	50 GeV $< m_{\mathrm{J}} < 270$ GeV

Chapter 5

Chapter name(demo)

Content of chapter
Content Content Content.

5.1 Section name

Content of section
Content Content Content

5.1.1 Subsection name

Content of subsection
Content Content Content

5.1.1.1 Subsubsection name

Content of subsubsection
Content Content Content

5.1.1.1.1 Paragraph name Content of paragraph
Content Content Content

Subparagraph name Content of subparagraph
Content Content Content

Chapter 6

Test demo

First line. (next line in $\LaTeX$)still first line.

Second line.

Chapter 7

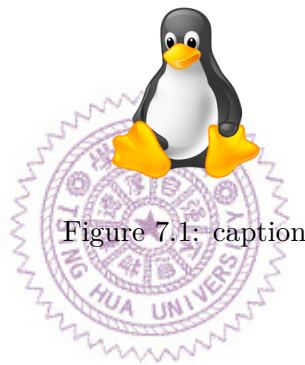# figure

7.1 Insert single figure(by sppmg's tool)

Figure 7.1: caption

7.2 Insert figures
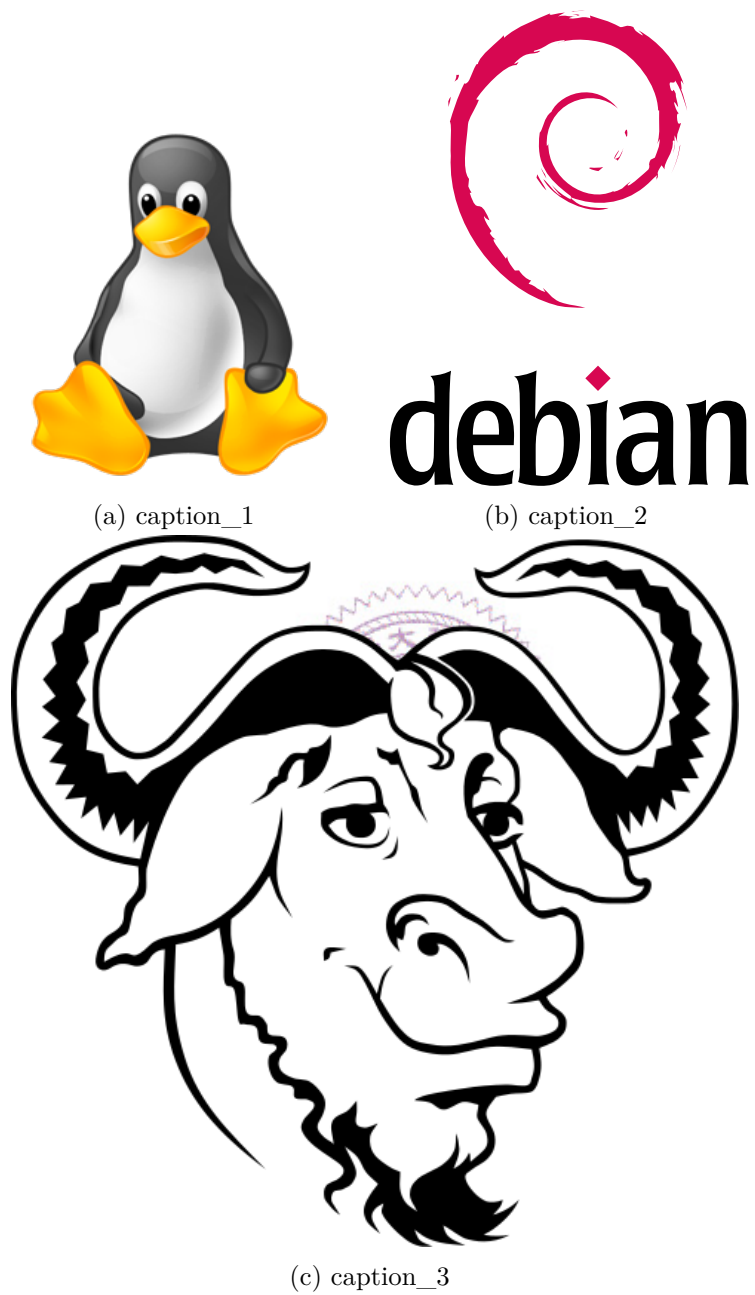
(a) caption_1

(b) caption_2

(c) caption_3

Figure 7.2: caption, use "(b)" get ID of subfigure(this ID is Debian) in caption

Chapter 8

Table

8.1 Simple table

Table 8.1: Solution

Component	Concentration(mM)
CaCl$_2$	118.0

8.2 Auto break line table

short	short short
long	long long long long long long long long long long

Appendix A

List of device

Table A.1: List of device

device	Model	Description
Linux	Debian 9	Best of best of best OS
Windows	10	Best of Best tool to prevent the aging of brain.

APPENDIX A. LIST OF DEVICE

Appendix B

Solutions

B.1   The solution

Table B.1: The solution

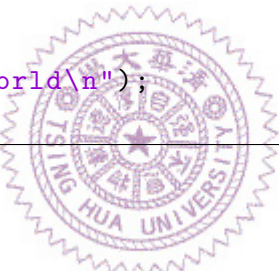| Component	Concentration(mM)
NaCl	1.0
CaCl$_2$	2.0
NaCl	1.0
CaCl$_2$	2.0

Appendix C

Code

C.1 C

Code C.1: hello_world_c.c

```c
#include <stdio.h>
main()
{
    printf("hello, world\n");
}
```

C.2 Matlab

Code C.2: hello_world_matlab.m

```matlab
fprintf('hello, world\n');
```

C.3 IDL

Code C.3: hello_world_idl.pro

```idl
print,"hello, world"

end
```